BBA - Molecular and Cell Biology of Lipids 1865 (2020) 158739

Contents lists available at ScienceDirect

BBA - Molecular and Cell Biology of Lipids

journal homepage: www.elsevier.com/locate/bbalip

Olesoxime, a cholesterol-like neuroprotectant restrains synaptic vesicle exocytosis in the mice motor nerve terminals: Possible role of VDACs

Guzalia F. Zakyrjanova[a,b], Amir I. Gilmutdinov[a], Andrey N. Tsentsevitsky[a], Alexey M. Petrov[a,b,*]

[a] Laboratory of Biophysics of Synaptic Processes, Kazan Institute of Biochemistry and Biophysics, Federal Research Center "Kazan Scientific Center of RAS", 2/31 Lobachevsky Street, box 30, Kazan 420111, Russia

[b] Institute of Neuroscience, Kazan State Medial University, 49 Butlerova Street, Kazan 420012, Russia

ARTICLE INFO

Keywords:
Olesoxime
Synaptic vesicle
Voltage dependent anion channels
Neuromuscular junction
Neurotransmitter release
Chloride permeability

ABSTRACT

Olesoxime is a cholesterol-like neuroprotective compound that targets to mitochondrial voltage dependent anion channels (VDACs). VDACs were also found in the plasma membrane and highly expressed in the presynaptic compartment. Here, we studied the effects of olesoxime and VDAC inhibitors on neurotransmission in the mouse neuromuscular junction. Electrophysiological analysis revealed that olesoxime suppressed selectively evoked neurotransmitter release in response to a single stimulus and 20 Hz activity. Also olesoxime decreased the rate of FM1–43 dye loss (an indicator of synaptic vesicle exocytosis) at low frequency stimulation and 20 Hz. Furthermore, an increase in extracellular Cl^- enhanced the action of olesoxime on the exocytosis and olesoxime increased intracellular Cl^- levels. The effects of olesoxime on the evoked synaptic vesicle exocytosis and $[Cl^-]_i$ were blocked by membrane-permeable and impermeable VDAC inhibitors. Immunofluorescent labeling pointed on the presence of VDACs on the synaptic membranes. Rotenone-induced mitochondrial dysfunction perturbed the exocytotic release of FM1–43 and cell-permeable VDAC inhibitor (but not olesoxime or impermeable VDAC inhibitor) partially mitigated the rotenone-driven alterations in the FM1–43 unloading and mitochondrial superoxide production. Thus, olesoxime restrains neurotransmission by acting on plasmalemmal VDACs whose activation can limit synaptic vesicle exocytosis probably via increasing anion flux into the nerve terminals.

1. Introduction

Synaptic transmission relies on exocytotic neurotransmitter release from synaptic vesicles (SVs). To maintain neurotransmitter release after exocytosis, the SV membrane is retrieved by endocytosis and newly formed vesicle is refilled with neurotransmitter and recruited into the SV pool. The reuse of SV membrane guarantees a reliability of neurotransmission and its relative independence from delivery of SV material from the neuronal soma [1,2]. Many signaling molecules and ion channels regulate neurotransmitter release, acting directly on exocytotic machinery or other steps of SV cycling. Also, some potent neurotoxins specifically affect presynaptic machinery mediating SV fusion or interfere with neurotransmitter release indirectly [3–5]. Several autoimmune antibodies target motor nerve terminals causing acute or long-lasting defects in neurotransmission and, hence, motor deficit [3]. Generally, disturbances of neurotransmitter release regulation occur in numerous pathological conditions, including early stages of neurodegenerative diseases [6–8]. The resulting aberrant neurotransmission can contribute to progression of the disorders [8–10]. Accordingly, pharmacological compounds able to balance a neurotransmitter release can be useful tools for a disease-modifying treatment [11].

Neurotransmitter release and SV cycling are tightly dependent on membrane cholesterol levels, because cholesterol is a partner for many synaptic proteins and essential for membrane deformations [9,12]. Partial cholesterol depletion suppresses evoked and increases spontaneous neurotransmitter release in CNS and neuromuscular synapses [13–18]. Extraction of cholesterol from SV membranes arrests endocytosis and recycling [19–21]. Furthermore, cholesterol metabolites at low submicromolar concentrations as well as cholesterol oxidation can affect neurotransmitter release and properties of the synaptic

Abbreviations: Chloride ion, Cl^-; 4,4′-Diisothiocyanatostilbene-2,2′-disulfonate, DIDS; end plate potentials, EPPs; miniature end plate potentials, MEPPs; neuromuscular junctions, NMJs; reactive oxygen species, ROS; S-18 phosphorothioate randomer oligonucleotide, S-18; synaptic vesicles, SVs; voltage dependent anion channels, VDAC

* Corresponding author at: Laboratory of Biophysics of Synaptic Processes, Kazan Institute of Biochemistry and Biophysics, Federal Research Center "Kazan Scientific Center of RAS", 2/31 Lobachevsky Street, box 30, Kazan 420111, Russia.

E-mail address: aleksey.petrov@kazangmu.ru (A.M. Petrov).

https://doi.org/10.1016/j.bbalip.2020.158739
Received 18 March 2020; Received in revised form 11 May 2020; Accepted 13 May 2020
Available online 16 May 2020
1388-1981/

membranes [12,22]. Indeed, brain-derived cholesterol metabolite 24-hydroxycholesterol modulates SV recruitment to exocytosis via dependent on glutamate NMDA or liver X receptor pathways [23–25]. An intermediate product in cholestanol biosynthesis 5α-cholestan-3-one decreased the number of SVs participating in *exo-* and endocytosis during prolonged activity [26,27]. The levels of the oxysterols and neuronal membrane cholesterol change in many pathological conditions, suggesting that cholesterol-dependent modulation contributes to synaptic dysfunction [10,28–33]. Therefore, intervention in cholesterol homeostasis and using cholesterol-like molecules may be considered as possible therapeutic approaches able to normalize synaptic transmission.

Cholest-4-en-3-one, oxime (olesoxime or TRO19622) is a cholesterol derivative which is considered as promising therapy for neurodegenerative disorders, including amyotrophic lateral sclerosis, peripheral neuropathy, spinal muscular atrophy, Huntington's and Parkinson's diseases [34,35]. Previously, we found that olesoxime can modulate neurotransmission in the frog neuromuscular junctions (NMJs), but the underlying mechanism was not identified [26]. Theoretically, the synaptic mechanism can contribute to neuroprotective properties of olesoxime and represent a new pathway for regulation of neurotransmission by cholesterol-like molecules. Olesoxime targets to voltage-dependent anion channels (VDACs) in the outer mitochondrial membrane and this interaction is required for inhibition of mitochondrial permeability transition pore complex, oxidative stress and apoptosis [34–38]. Also, VDACs are localized in the neuronal plasma membrane, particularly in cholesterol-rich microdomains [39–45]. Functions of plasma membrane VDACs could be linked with control of anion permeability, cell volume, apoptosis, amyloid toxicity, redox status and estrogen receptor α-dependent signaling [39–44,46–48]. Furthermore, VDACs have been detected in proteome of the presynaptic membrane, active zones and SVs [49–53]. However, significance of VDACs for presynaptic function has not been studied so far. At the same time, fundamental role of VDAC in many cellular processes implies a possible relevance for neurotransmission, specifically regulation of neurotransmitter release.

In the present work, for the first time we studied the mechanism by which olesoxime can modulate neurotransmission in mammalian NMJs. Furthermore, a potential role of plasmalemmal VDACs and VDAC-associated Cl^- transport in the effects of olesoxime were in the focus of the work. We revealed that olesoxime restricted the neurotransmitter release and translocation of SVs to exocytotic sites during activity in the mice NMJ. Also olesoxime increased intracellular Cl^- levels. These effects of olesoxime were suppressed by cell-permeable and -impermeable inhibitors of VDACs. Furthermore, the olesoxime effect on the exocytosis was enhanced by an increase in extracellular Cl^- levels. These results indicate that plasma membrane VDACs can negatively modulate neurotransmission via enhancing Cl^- transport and olesoxime can trigger this new mechanism of neurotransmitter release regulation.

2. Material and methods

2.1. Animals

The isolated phrenic nerve-diaphragm preparations from adult mice were used in the experiments. Animals were maintained at a 12-h light/12-h dark cycle; water and food were provided ad libitum. Mice (4–6 months of age) were anesthetized using an intraperitoneal injection of Na^+ pentobarbital (40 mg/kg) and decapitated with a guillotine; the diaphragm with nerve stub was quickly excised. The protocol was approved by the Bioethics Committees of Kazan Medical University and met the requirements of the EU Directive 2010/63/EU as well as European Convention for the Protection of Vertebrate Animals used for Experimental and other Scientific Purposes (Council of Europe No 123, Strasbourg, 1985).

2.2. Solutions and chemicals

The nerve hemidiaphragm preparations were pinned to the bottom of Sylgard-coated chambers. The muscles were perfused at 5 ml·min^{-1} with physiological solution (129 mM NaCl, 5 mM KCl, 2 mM $CaCl_2$, 1 mM $MgSO_4$, 1 mM NaH_2PO_4, 20 mM $NaHCO_3$, 11 mM glucose and 3 mM HEPES; pH – 7.4) saturated with a 5% CO_2/95% O_2 gas mixture. In some experiments a solution with high Cl^- concentration (146 mM NaCl, 5 mM KCl, 2 mM $CaCl_2$, 1 mM $MgCl_2$, 13.5 mM CholineCl and 3 mM HEPES; pH – 7.4) was used.

Pretreatment with 0.4 μM olesoxime (Tocris) lasted 20 min prior to the nerve stimulation at 20 Hz or 5 Hz. Olesoxime was dissolved in DMSO (Tocris) and final concentration of the vehicle was 0.001%. At a concentration of 0.001–0.1% DMSO did not affect neuromuscular transmission in the mice diaphragm [23–25], thence the data from DMSO experiments were used as controls. DIDS (50 μM, 4,4′-Diisothiocyanatostilbene-2,2′-disulfonate; Tocris) [54,55] and S-18 (1 μM, S-18 phosphorothioate randomer oligonucleotide; Trilink) [56,57] were used as inhibitors of VDACs and added to the bathing solution 5 min before the application of olesoxime and remained in the perfusion throughout the experiment. Rotenone (10 μM, a 30 min-application; Sigma) was used to induce mitochondrial dysfunction [58]. (−)Vesamicol (2 μM, Sigma) was used as inhibitor of vesicular acetylcholine transporter which is responsible for refilling of SVs with acetylcholine [59].

2.3. Postsynaptic potential recordings

End-plate potentials (EPPs) and miniature EPPs (MEPPs) were recorded using standard intracellular glass microelectrodes filled with 2.5 M KCl (tip resistance 5–10 MΩ). For the signal detection a Model 1600 amplifier (A-M System) and LA II digital I/O board (Pushino, Russia) were used. The recorded signals were filtered between 0.03 Hz and 10 kHz, digitized at 50 kHz and stored on PC for off-line analysis. Data were processed using a custom-developed program [60] and analyzed to estimate mean amplitudes, rise (from 20% to 80% of the peak amplitude) and decay (from peak to 50% of the peak amplitude) times. The frequency of MEPPs was estimated in experiments after recording 150–200 signals. For MEPPs signal-to-noise ratio was > 7:1 and threshold for the MEPP detection was set at level of 0.2 mV. The nerve was stimulated by rectangular supramaximal electrical 0.1-ms pulses at a frequency of 0.5 Hz or 20 Hz with a suction electrode connected to an isolated stimulator Model 2100 (A-M Systems, USA). To prevent muscle contractions, the muscle-specific Na^+ channel inhibitor μ-conotoxin-GIIIB (0.5 μM; Alamone Lab) was added to the perfusion 20 min prior to recording. EPPs were recorded at low frequency (0.5 Hz) stimulation during 20-min olesoxime treatment, and then 20 Hz stimulation was applied for 3 min to the phrenic nerve of the pretreated with olesoxime muscles.

2.4. Optical approaches

Images were recorded using a microscope (BX51WI Olympus) equipped with confocal spinning disk confocal unit (Olympus) and UPLANSapo 60xw/LumPlanPF 100xw objectives. Images were captured by CCD-camera DP71 (Olympus) under control of CellSens software (Olympus). ImagePro (Media Cybernetics) was used for image analysis.

To estimate the rate of SV exocytosis FM1–43 dye (7 μM; Thermo Fisher) was used. This dye reversibly binds to the presynaptic membranes and is then captured by SV endocytosis [61]. To load SVs with FM1–43, the phrenic nerve was stimulated at 20 Hz for 3 min or 5 Hz for 10 min. The preparations were exposed to FM1–43 during the stimulation and 5 min after end of the stimulation, and then perfused with dye-free saline containing 30 μM ADVASEP-7 (Biotium) for 20 min to facilitate the removal of FM1–43 from the surface membranes. After exposure of the preparations to the drugs, the phrenic nerve was re-

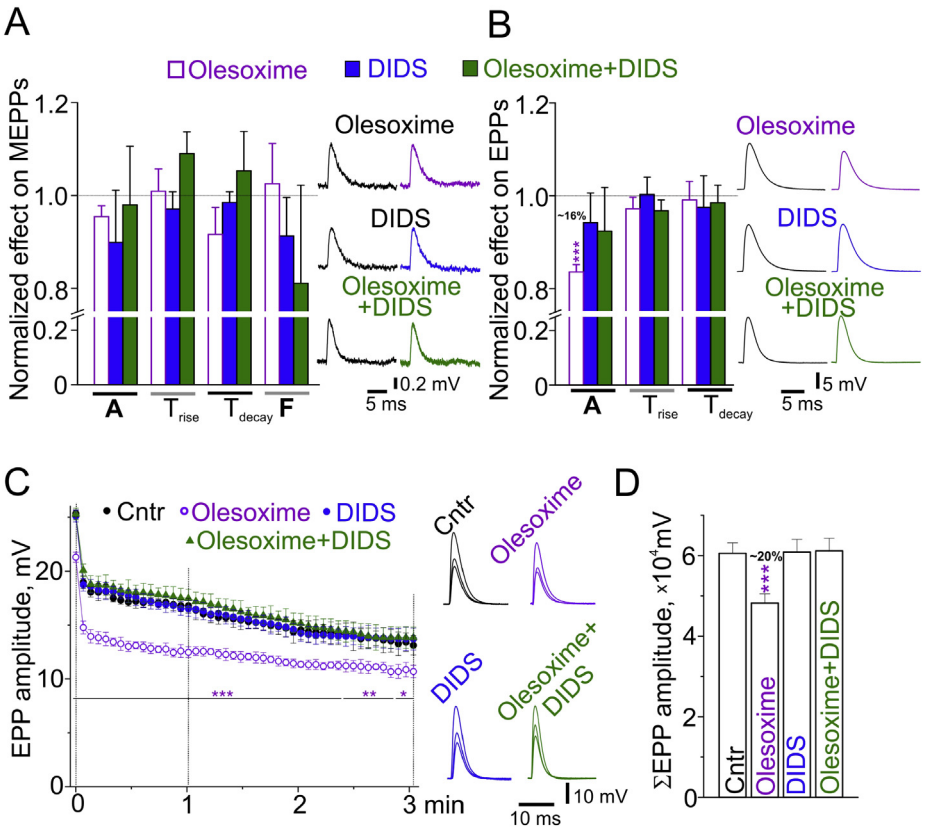

Fig. 1. Spontaneous and evoked neurotransmitter release: effects of olesoxime and VDAC inhibitor DIDS. A, B - the histogram showing the effect of the drugs on peak amplitude (A), rise time (T_{rise}), decay time (T_{decay}) and frequency (F) of MEPPs (A) and on peak amplitude, rise and decay time of EPPs (B). EPPs were evoked by stimulation at 0.5 Hz. Y-axis indicates the normalized effect of the drugs (1.0 - is a value before application of the drugs). A, B- right, representative MEPPs (A) and EPPs (B) before and 20 min after (in color) exposure to the drugs. C – Depression of EPP amplitude (in mV) at 20 Hz stimulation in control and drug-pretreated muscles. Right, typical EPPs at 0, 1, 3 min of 20 Hz stimulation. D - The histogram showing cumulative EPP amplitudes (in mV; from C) at 20 Hz stimulation. A-D - All results are the mean ± SEM of the measurements in individual mice (n = 8–11 per group). *P<0.05, **P<0.01, ***P<0.001 – by a two-tailed unpaired t-test (B) or a repeated ANOVA followed by the Bonferroni post-hoc (C). Numbers above the boxes represent a decrease (in %) in mean value compared to value before drug application (B) or value in control group (D).

stimulated at 20 Hz or 5 Hz for 10 min to evoke SV fusion, leading to a decrease in the nerve terminal fluorescence (unloading). The images were recorded before the onset of stimulation (0) and at different time points (5, 10, 15, 20, 25, 30, 45, 60, 90, 120, 150, 180, 240, 300, 420, 600 s) during the stimulation. The regions of interest were illuminated only at moments of the image capturing. The fluorescence of FM1–43 was detected using a 480/10 nm excitation filter, a 505 nm dichroic mirror and a 535/40 nm emission filter. Background signal was estimated as the mean intensity of fluorescence in a region outside of the NMJs (4x30 μm^2). Nerve terminal signal was determined as the average pixel intensity in regions of interest after background value subtraction [62]. To illustrate the rate of the dye loss, the initial value of nerve terminal signal (before the onset of stimulation) was taken as 1.0.

For immunofluorescent staining, the muscles were fixed with 3.7% p-formaldehyde for 40 min, permeabilized with 1% Triton X-100 in PBS for 30 min and then incubated in blocking buffer (2% normal goat serum, 0.1% Triton X-100, 0.05% Tween 20 and 1% BSA in PBS) for 1 h [17]. The fixed samples were incubated with primary rabbit anti-VDAC antibody (1:400; #V2139, Sigma) and a marker for junctional region (1 ng/ml rhodamine-conjugated α-bungarotoxin; Molecular Probes) at 4 °C overnight. Exposure to secondary AlexaFluor 488-conjugated anti-rabbit antibody (1:1000, Abcam) lasted 1 h. All procedures were performed at room temperature excluding incubation with the primary antibodies. The primary and secondary antibodies were diluted in PBS containing 1% BSA, 0.05% Triton X-100 and 0.05% Tween 20. After each step of the immunolabeling procedure the muscles were washed four times with PBS for 1.5 h. No fluorescent staining of VDAC was detected without addition of the primary antibody. AlexaFluor 488 (rhodamine) fluorescence was excited by a light of 480 nm (555 nm) wavelength and emission was recorded using a band-pass filter of 530/15 nm (630/20 nm).

MitoSox was used as indicator of reactive oxygen species (ROS) within the mitochondria. The dye is selectively accumulated in the mitochondria and emits a red fluorescence after oxidation by superoxide. The preparations were incubated with 2 μM MitoSox for 15 min and then perfused with a physiological saline (dye-free) for 40 min [63]. Fluorescence was visualized using a 510/10 nm excitation filter and a 590/20 nm emission filter.

Changes in intracellular Cl^- levels were visualized using a MEQ (AAT Bioquest). MEQ fluorescence was excited by a 360–370 nm wavelength light and detected using a 420IF emission filter; a 410 nm dichroic mirror was used. MEQ fluorescence is markedly quenched in a concentration-dependent manner by Cl^- without shifting the emission spectra [64,65]. To load the dye into nerve terminals MEQ was applied for 3 h to the cut end of phrenic nerve (about 2 mm in length) using suction pipette tip filled with the dye (50 mM in PBS). During the incubation period the dye molecules entered into the axons and carried to the presynaptic terminals. Then the phrenic nerve was removed from the suction pipette by applying weak positive pressure and the preparations were perfused for 20 min with physiological saline. The stump of the nerve was reintroduced into the dye-free suction electrode to avoid the dye leakage. The analysis of MEQ fluorescence intensity was performed in NMJs. The value of the initial nerve terminal fluorescence was taken as 0.0. To control photobleaching of MEQ, the fluorescence was recorded without stimulation at the same conditions of illumination as when the nerve hemidiaphragm preparations were stimulated at 20 Hz.

2.5. Statistical analysis

Statistical analysis was performed with Origin Pro 9.2 software, using significance levels of 0.05, 0.01 and 0.001. Either a two-tailed t-test or repeated two-way ANOVA followed by the Bonferroni post-hoc were used. The data are presented as Mean ± SEM, where n is the number of independent experiments on different mice; n is indicated in each figure legend.

3. Results

3.1. Influence of VDAC modulators on spontaneous and evoked neurotransmitter release

Postsynaptic potentials reflecting spontaneous (MEPPs) and evoked (EPPs at 0.5 Hz) acetylcholine release were recorded before and after 20 min application of drugs (Fig. 1). Resting membrane potential was constant under these conditions. Olesoxime (0.4 μM) did not change MEPP parameters, namely amplitude, rise time, decay time and frequency (Fig. 1A). Similarly DIDS, an inhibitor of anion transport, including VDAC activity [54,66], had no effects on the MEPP parameters. Co-application of olesoxime and DIDS did not modify the MEPPs (Fig. 1 A). Olesoxime statistically significant decreased EPP amplitude at low frequency stimulation (0.5 Hz), without affecting rise and decay time of the EPP (Fig. 1B). DIDS itself did not change EPP amplitude, but prevented the depressant effect of olesoxime. Note that olesoxime at higher concentrations reduced EPP amplitudes (without affecting MEPP amplitudes) to the similar degree as 0.4 μM (Suppl. Fig. 1A,B), suggesting that the effect of 0.4 μM olesoxime was close to maximal.

Stimulation of motor nerve at higher frequency leads to mobilization of SVs from the recycling and reserve pools [67,68]. During prolonged 20 Hz stimulation, the efficiency of neurotransmitter release is dependent on the transport of SVs to the active zone and their recycling during continuous activity. 20-Hz stimulation led to a biphasic change in the EPP amplitude: after initial rapid decrease the amplitude continued to decline but at a slower rate. Pretreatment with olesoxime for 20 min caused a more profound decrease in the EPP amplitude, especially marked in the beginning period (Fig. 1C; Suppl. Fig. 1C). As a result, cumulative EPP amplitude was decreased to ~80% ($P < 0.001$) compared to the control, suggesting that olesoxime suppresses evoked neurotransmitter release at 20 Hz activity (Fig. 1D). DIDS itself did not modify the rate of the EPP amplitude depression during 20 Hz stimulation, but prevented the effect of olesoxime (Fig. 1 C, D; Suppl. Fig. 1C). Thus, olesoxime suppresses selectively evoked neurotransmitter release in response to low frequency (0.5 Hz) and 20 Hz stimulation without affecting spontaneous release. These effects of olesoxime were blocked by antagonist of VDACs.

3.2. FM1–43 unloading kinetics

Nerve terminals were loaded with FM1–43 by 20 Hz stimulation for 3 min (see Methods for details) and after 50 min-rest interval the phrenic nerves were re-stimulated at 20 Hz. This stimulation leads to decrease in the fluorescence (unloading) that reflects the release of the dye from the SVs by exocytosis (Fig. 2A). Olesoxime decreased the rate of the dye unloading. The slowdown of FM1–43 unloading was clearly expressed in the first minutes of the activity (Fig. 2A). DIDS itself did not change the dye loss at 20 Hz stimulation, but it completely prevented the effect of olesoxime on the FM1–43 unloading (Fig. 2B). This indicates that olesoxime attenuates SV exocytosis during the stimulus train and it can be dependent on a target that is sensitive to DIDS. DIDS effectively inhibits VDAC channel activity in different cell types and can affect both VDAC localized in mitochondria as well as plasma membrane [66,69]. To test the implication of plasma membrane VDACs in the effect of olesoxime on SV exocytosis, we used S-18 phosphorothioate randomer oligonucleotide (S-18) (Fig. 2C), which specifically blocks plasmalemmal VDAC and cannot pass through the cell membranes [56,57]. S-18 itself and in combination with DIDS had no influence on FM1–43 unloading, but S-18 completely prevented the effect of olesoxime.

Neurotransmission in physiological conditions mainly relies on reuse of SVs belonging to the small recycling pool. This pool participates in neurotransmitter release during initial period of prolonged 20 Hz stimulation and can continuously maintain neurotransmission at lower frequencies (< 10 Hz) of stimulation in the NMJs [67,70]. Olesoxime had more visible effect on both EPP amplitude and FM1–43 loss specifically during the first minutes of 20 Hz stimulation. This suggests that olesoxime can reduce the recruitment of SVs from recycling pool to active zone. Consistent with this is that olesoxime decreased the rate of the unloading at 5 Hz activity (Fig. 2D) and this effect of olesoxime was completely prevented by S-18, while S-18 itself had no influence on the dye unloading at 5 Hz (Fig. 2E). Electrophysiological experiments with an inhibitor of SV refilling with neurotransmitter vesamicol [59] also suggest that olesoxime can suppress neurotransmitter release from the recycling SVs, whose contribution to neurotransmitter release is dependent on re-loading of neurotransmitter during activity (Suppl. Fig. 2). Indeed, vesamicol enhanced a rundown of EPP amplitude at 20 Hz and in vesamicol-treated muscles, olesoxime had no profound additional effect on the depression of EPP amplitude (Suppl. Fig. 2B). As a result, cumulative EPP amplitudes (after 3 min of 20 Hz activity) were similar in vesamicol and olesoxime + vesamicol groups (Suppl. Fig. 2C).

Thus, olesoxime attenuates SV exocytosis at both 5 and 20 Hz activity. Furthermore, this action of olesoxime is prevented by cell-impermeable VDAC blocker S-18. Accordingly, the main target of olesoxime could be VDAC localized at the plasma membrane. Immunofluorescent labeling showed the presence of VDAC in NMJs (Fig. 2F), and a pattern of the immunofluorescence indicates on the plasma membrane expression of VDACs.

3.3. Mitochondria in the effect of olesoxime on SV exocytosis

Cellular effects of olesoxime can be linked with mitochondrial function. Rotenone induces mitochondrial dysfunction by inhibiting electron transport chain complex I, leading to ATP depletion, ROS production, decrease of cytosolic Ca^{2+} uptake, mitochondrial permeability transition pore opening and the loss of mitochondrial membrane potential [58,71,72]. Indeed, 30-min application of 10 μM rotenone led to increase in MitoSox fluorescence, an indicator of mitochondrial ROS production (Fig. 3A). This enhancement of MitoSox fluorescence can be partially inhibited by membrane-permeable DIDS, but not olesoxime or cell-impermeable S-18. Rotenone profoundly inhibited the FM1–43 unloading at 20 Hz (Fig. 3B), olesoxime and S-18 did not modify the effect of rotenone. At the same time, DIDS partially attenuated the effect of rotenone on both MitoSox fluorescence and FM1–43 unloading (Fig. 3C). It should be noted that rotenone increased frequency of MEPPs and destaining of FM1–43 in rest conditions (without stimulation), indicating on enhancement of spontaneous exocytosis (Suppl. Fig. 3A, B). In addition, rotenone slightly decreased amplitude of EPP at 0.5 Hz (Suppl. Fig. 3C) and markedly increased the depression of EPP amplitude during 20 Hz activity (Suppl. Fig. 3D, E). The effects of rotenone on both spontaneous release and rundown of EPPs at 20 Hz were not sensitive to olesoxime (Suppl. Fig. 3A, B, D, E, F). Thus, acute application of olesoxime cannot prevent the rotenone-induced mitochondrial ROS production and disturbance of SV exocytosis. These results suggest a mitochondria-independent action of olesoxime on exocytosis in the NMJs.

3.4. Anion (Cl^-)-dependence of olesoxime effects

Increase in Cl^- concentration in the bathing solution (by ~15%) decreased the FM1–43 unloading at 20 Hz stimulation (Fig. 4A). The depressant effect of olesoxime on the FM-43 unloading was markedly enhanced in the solution containing high Cl^- concentration (Fig. 4A). Along the same lines, the elevation in extracellular Cl^- levels enhanced rundown of EPP amplitude in response to high-frequency stimulation and the depressant effect of olesoxime on EPP amplitude at 20 Hz stimulation was markedly increased in the presence of high Cl^- solution (Suppl. Fig. 4). Accordingly, olesoxime and increase in extracellular Cl^- concentration had the similar depressant effects on SV exocytosis during 20 Hz activity. Furthermore, an increase in external Cl^- levels

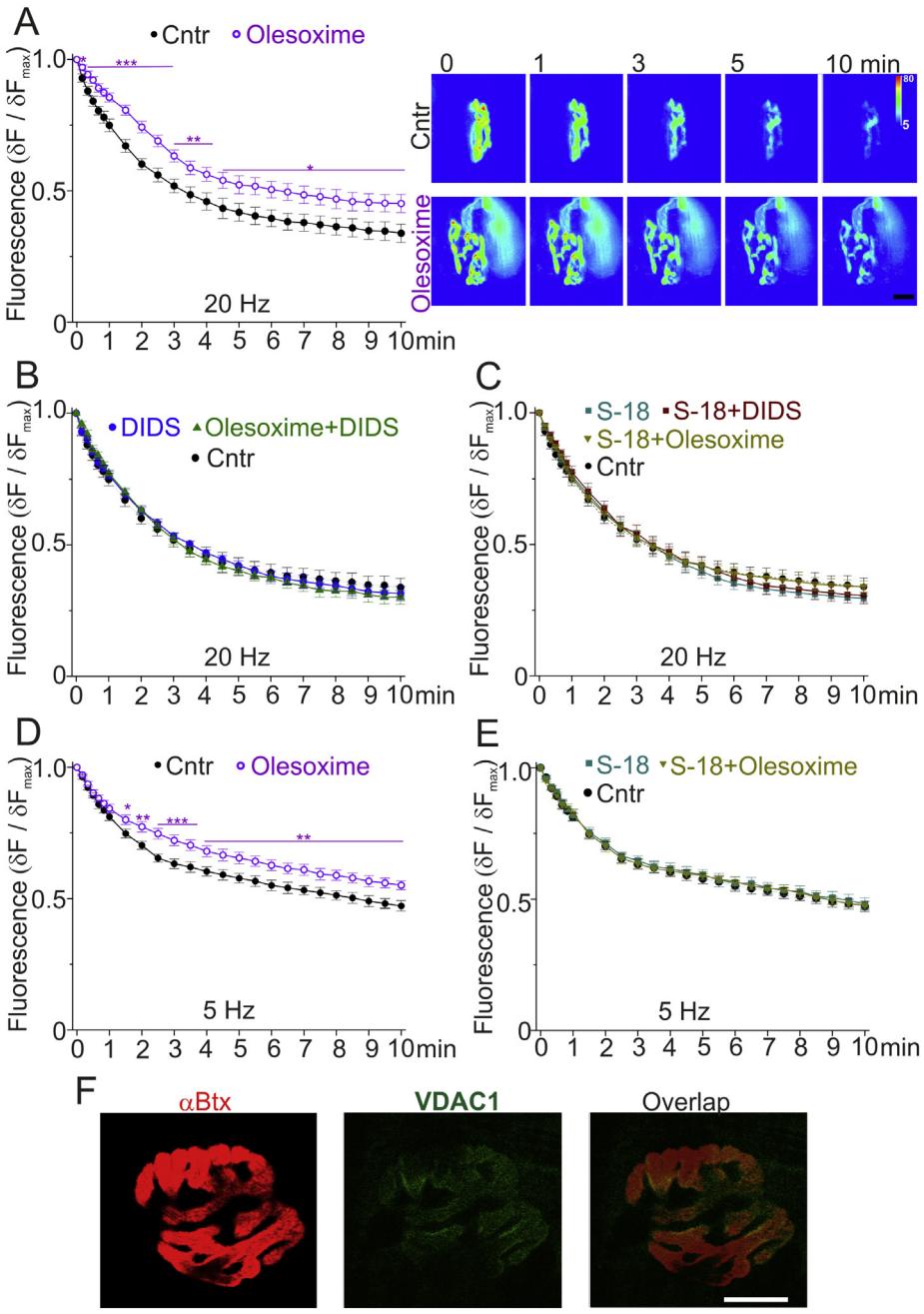

Fig. 2. FM1–43 dye unloading and the effects of VDAC modulators. A-E – Time course of FM1–43 dye loss during 20 Hz (A-C) and 5 Hz (D, E) stimulation. After the treatment with drugs, the dye-preloaded NMJs were re-stimulated (20 Hz or 5 Hz) to induce exocytosis which leads to release both neurotransmitter and FM1–43 molecules from SVs. A, D - Effect of olesoxime. A, Right, pseudo-color images of NMJs prior to 20 Hz stimulation (0) and at different times (in min) during the stimulation; the corresponding intensity scale is provided to the right (a.u.). Scale bar – 10 μm. B – Influence of DIDS itself and in combination with olesoxime. C, E - Influence of S-18 itself and in combination with olesoxime. The control FM1–43 unloading curves are shown in B, C, E as dashed curves. A-E, Y-axis – the fluorescence intensity (δF/δFmax), relative to the value prior to the onset of the stimulation at 20 Hz (A-C) or 5 Hz (D, E). Mean ± SEM; $n = 12$ for each group. *P<0.05, **P<0.01, ***P<0.001 – by a repeated ANOVA followed by the Bonferroni post-hoc. F- Immunolocalization of VDACs in the NMJ. The representative image of NMJ double-stained with anti-VDAC antibody and rhodamine-conjugated α-bungarotoxin/αBtx (to label junctional nicotinic acetylcholine receptors). In the overlapping image, the intensity of red channel (αBtx) was decreased. Scale bar – 10 μm.

augmented the ability of olesoxime to depress exocytotic neurotransmitter release. The negative effect of olesoxime was reduced by S-18, an inhibitor of plasmalemmal VDACs (Fig. 4B).

To estimate change in intracellular Cl^- levels, the nerve terminals were loaded with fluorescent Cl^- indicator MEQ, which fluorescence is quenched by Cl^- [64,65]. The nerve terminal fluorescence was relatively stable at rest conditions and fluorescence increased in response to exposure to solution containing lower Cl^- concentration (due to using Na^+-gluconate instead of NaCl in physiological saline). This points on a sensitivity of MEQ dye loaded into nerve terminal to change in Cl^- levels. Olesoxime slightly and transiently decreased MEQ fluorescence at rest conditions (Fig. 4C). This effect of olesoxime was prevented by VDAC inhibitors (DIDS and S-18). By itself DIDS and S-18 had no influence on the fluorescence (Fig. 4D). Stimulation at 20 Hz slightly decreased the MEQ signal; olesoxime caused a more significant drop of the fluorescence during the stimulus train (Fig. 4E). VDAC inhibitors prevented this action of olesoxime, while DIDS or S-18 individually did not modify time course of the MEQ fluorescence at 20 Hz activity (Fig. 4F). Therefore, olesoxime can increase presynaptic membrane permeability for Cl^- at both rest conditions and during synaptic activity; and this action of olesoxime is dependent on VDACs.

4. Discussion

Exocytotic neurotransmitter release is tightly regulated event that determines the efficiency of synaptic transmission. Numerous ion channels and receptors are involved in modulation of SV exocytosis and vesicular transport. Furthermore, several potent neurotoxins and autoantibodies specifically affect neurotransmitter release [3,5]. The main findings of the present study are: presynaptic membrane VDAC activity can control SV exocytosis and Cl^- flux into the motor nerve terminals; a neuroprotective molecule olesoxime limits exocytotic neurotransmitter release by activating the plasmalemmal but not mitochondrial VDAC channel activity (Fig. 5).

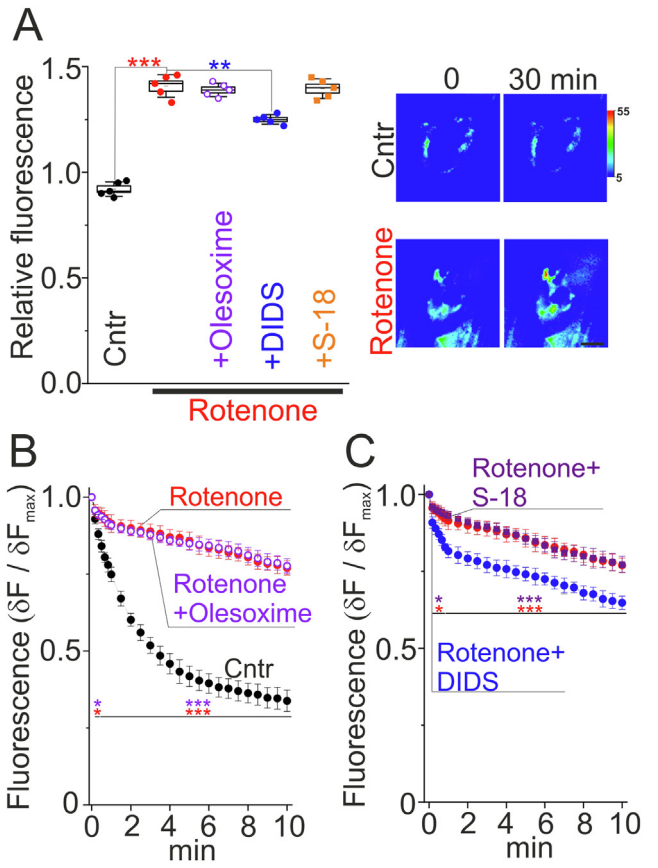

Fig. 3. Role of mitochondria in the effects of VDAC modulators. A - Mitochondrial superoxide production in the NMJ. Changes in MitoSox fluorescence in response to application of a mitochondrial poison rotenone itself and in combination with VDAC modulators are shown. Y-axis – relative fluorescence, where 1.0 – is value prior to application of the drug or vehicle (Cntr). Mean ± SEM; $n = 5$ for each group. **P<0.01, ***P<0.001 – by a two-tailed unpaired *t*-test. Right, pseudo-color images prior to and 30 min after exposure to vehicle or rotenone; the corresponding intensity scale is provided to the right (a.u.). Scale bar – 10 μm. B, C – Effect of rotenone itself and in combination with VDAC modulators on FM1–43 unloading during 20 Hz stimulation. The control FM1–43 unloading curve (from Fig. 2A) is shown in B as dashed curve. B, C - Y-axis – the fluorescence intensity (δF/δFmax), relative to the value before the onset of the stimulation. Mean ± SEM; n = 12 for each group. *P<0.05, ***P<0.001 – by a repeated ANOVA followed by the Bonferroni post-hoc.

Typically, VDACs represent integral membrane proteins forming pore for small hydrophilic molecules in the outer membrane of mitochondria [73,74]. However, several studies pointed on a localization of VDACs in the plasmalemma [39,42–45], including neuronal and synaptic plasma membranes [75–78]. Consistent with these studies, there was a pattern of VDAC immunolabeling observed in the NMJs. Omics approaches revealed that VDAC is a presynaptic active zone protein [49–51] and all three isoforms of VDACs were detected in fraction of docked SVs [49,52] as well as in SV membranes [53]. These data suggest a specific presynaptic role of plasmalemmal VDACs, which has not yet been identified. High levels of cholesterol in nerve terminal and SV membranes [12] can be one of mechanism for anchoring VDACs into presynaptic membranes. Indeed, VDACs contain multiple cholesterol-binding sites [79,80] and preferentially reside in cholesterol-rich microdomains of the plasma membrane [40–43]. The observed non-uniform signal from immunolabeled VDAC could reflect clusterization of VDACs in lipid rafts or membrane contact sites of the NMJs. The latter are enriched with cholesterol-rich rafts, whose integrity is sensitive to nerve activity [12,81,82].

Herein, we revealed that VDAC-binding cholesterol-like molecule olesoxime [34,36,38] can suppress evoked exocytosis of SVs and their recruitment to exocytotic sites. This action of olesoxime was completely prevented by VDAC inhibitors, membrane-permeable DIDS [54,66] and impermeable S-18 [56]. Note that spontaneous neurotransmitter release was not affected by any of these VDAC modulators. Accordingly, we suggest that stimulation of plasmalemmal VDACs can specifically limit evoked neurotransmitter release by suppressing involvement of SVs in exocytosis. During moderate (physiological) activity neurotransmission mainly relies on exocytosis of SVs belonging to the recycling pool [67,70]. These SVs undergo multiple rounds of *exo*-endocytosis coupled to refilling with neurotransmitter during activity [67]. Olesoxime was able to suppress the rate of the SV exocytosis at moderate stimulation, and this effect of olesoxime was prevented by cell-impermeable VDAC inhibitor. Furthermore, if refilling of recycling SVs with acetylcholine was blocked by vesamicol, then olesoxime did not additionally suppress neurotransmitter release during prolonged activity. Hence, plasmalemmal VDACs can negatively regulate neurotransmission at physiological level of activity, which relies on synaptic vesicle recycling. This is in accordance with observation that flies lacking *porin* (homologs to mammalian VDACs) exhibit neurological dysfunction, aberrant electrophysiological response at the larval NMJs and skeletal muscle abnormality [73,83]. Note that significant increase in evoked postsynaptic potential (in the presence of low extracellular Ca^{2+}) and decrease in percentage of stimulation that failed to evoke the postsynaptic response were observed in the mutant flies [83]. This suggests that lack of VDACs can lead to hyperexcitability at the synaptic level. However, Graham at co-authors linked the observed alterations with a paucity of mitochondria in the presynaptic terminals due to disturbance of axonal mitochondrial trafficking [83]. Along the same line, many studies suggest that beneficial effects of olesoxime are realized via action on mitochondrial VDACs [34–36,38]. In the present work, we used model of rotenone-induce mitochondrial dysfunction which leads to opening of mitochondrial permeability transition pore and increase in mitochondrial ROS production [58,71]. Indeed, acute exposure to rotenone led to an increase in mitochondrial superoxide generation which was accompanied by a marked suppression of evoked SV exocytosis in the NMJs. Similarly, inhibition of mitochondrial complex I with rotenote caused a disturbance of SV exocytosis and recycling in synaptosomes and primary hippocampal culture [84–86]. Olesoxime or cell-impermeable VDAC inhibitor (S-18) cannot suppress the effects of rotenone on both ROS levels and SV exocytosis, while membrane-permeable VDAC antagonist DIDS partially attenuated the rotenone action. This is consistent with ability of DIDS to inhibit the rotenone-induced release of superoxide anion from the mitochondria matrix to cytosol through VDACs [87]. Probably, acute application of olesoxime can modulate SV exocytosis in mitochondria- and mitochondrial VDAC-independent manner. Consistent with this is that olesoxime did not prevent increase in spontaneous neurotransmitter release in response to rotenone application.

Theoretically, there are multiple mechanisms underlying the negative regulation of evoked SV exocytosis by plasmalemmal VDACs. These VDACs can serve as voltage-dependent Cl^- channels that can be activated by antiestrogens [42,43]. Also plasmalemmal VDACs can promote anion efflux in apoptotic neurons, but act as NADH (−ferricyanide) reductase thereby contributing to redox homeostasis in basal conditions [39,44]. VDACs can affect Ca^{2+} signaling and protein kinase (e.g. AKT, GSK3β) activity [47,48,88] as well as be a negative regulator of neuroprotective estrogen receptor α [40,41]. Finally, plasmalemmal VDAC can, directly or indirectly, contribute to ATP release from mammalian cells [89]. In the present study, we tested a hypothesis that olesoxime acting on VDACs can change anion (Cl^-) flux thereby affecting the SV exocytosis. Indeed, an increase in external Cl^- levels markedly enhanced the depressant effect of olesoxime on exocytosis, and under these conditions cell-impermeable VDAC blocker (S-18) completely prevented the action of olesoxime. Experiments with a Cl^- indicator MEQ loaded into the nerve terminals confirmed that

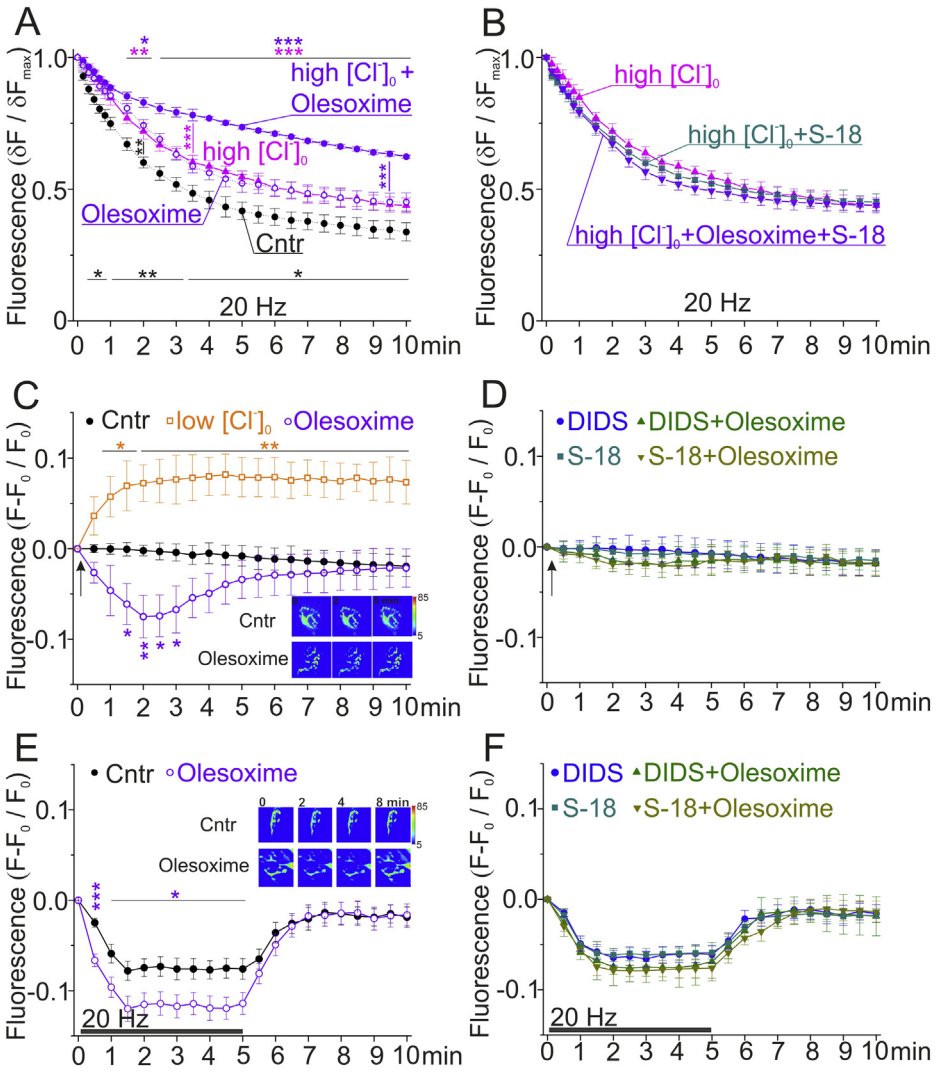

Fig. 4. Role of Cl^- in the effects of VDAC modulators. A, B – Effects of VDAC modulators (olesoxime and S-18) on FM1–43 unloading (at 20 Hz) in the presence of high extracellular Cl^- (high $[Cl^-]_o$). The FM1–43 unloading curves of control and olesoxime-treated muscle (from Fig. 2A) are shown in A as dashed curves. A, B, – Y-axis – the fluorescence intensity (δF/δFmax), where 1.0 represents the value before the 20 Hz stimulation. C–F, Changes of Cl^--sensitive dye (MEQ) fluorescence at rest (C, D) and during 20 Hz stimulation (E, F): effects of VDAC modulators. MEQ is loaded into the motor nerve terminals and its fluorescence is quenched by Cl^-. A decrease in extracellular Cl^- levels (low $[Cl^-]_o$) caused an increase in MEQ fluorescence (C). Acute exposure to olesoxime transiently decreased the MEQ signal (C). Furthermore, 20 Hz stimulation more markedly decreased MEQ fluorescence in olesoxime-pretreated muscles (E). C, E – Right, the pseudo-color images illustrating these changes in the intensity of fluorescence; the corresponding intensity scales are provided to the right (a.u.). D, F – Effects of olesoxime were not expressed in the presence of VDAC inhibitors (DIDS and S-18). Arrows (C, D) and horizontal thick lines (E, F) indicate moment of olesoxime addition and 20 Hz stimulus train, respectively. C–F - Y-axis - relative fluorescence intensity calculated according to eq. $(F-F_0)/F_0$, where F_0 is baseline fluorescence before olesoxime application (C, D) or the onset of 20 Hz stimulation (E, F). A-F, Mean ± SEM; n = 12 for each group. *P<0.05, **P<0.01, ***P<0.001 – by a repeated ANOVA followed by the Bonferroni post-hoc.

olesoxime can increase intracellular Cl^- levels at rest and during synaptic activity. Furthermore, VDAC inhibitors (DIDS and S-18) prevented the effects of olesoxime on the presynaptic Cl^- levels. Note that either S-18 or DIDS itself had no effect on SV exocytosis as well as cytosolic Cl^- content, suggesting that VDACs are not involved in control of neurotransmission in basal conditions without activation with exogenous or endogenous compounds. Conceivable, neuroactive steroids, plasminogen, tissue-type plasminogen activator (tPA) and ceramide can be natural ligands that can affect the plasmallemal VDAC activity [47,88,90,91]. It is tempting to speculate that VDACs can serve as an ionotropic presynaptic receptor responsible for negative regulation of SV exocytosis due to the increased Cl^- conductance during activity. Accordingly, some neuroprotective properties of olesoxime [34–36] could be attributed to effects on the presynaptic VDACs and prevention of excess neurotransmitter release. The latter can cause synaptic damage in both central synapses and NMJs during pathologic processes, including neurodegenerative disorders (e.g. Alzheimer's disease) and poisoning with several neurotoxins [3,5,7,92–94]. Theoretically, target delivery of olesoxime and other therapeutic compounds to synaptic compartment could be achieved by using liposomes coupled to atoxic forms of highly neurotropic tetanus and botulinum neurotoxins [95–97].

5. Conclusion

In sum, we suggest that presynaptic membrane VDACs can negatively regulate neurotransmission by suppressing evoked exocytosis of SVs and their recruitment to exocytotic sites. The mechanism underlying VDAC-dependent regulation of neurotransmitter release could be linked with increase in permeability of the presynaptic membrane to anion (Cl^-). Plasmalemmal VDAC-mediated depression of neurotransmission can be triggered by a cholesterol-like neuroprotectant olesoxime. Limitation of the present study is the use of pharmacological approaches to modulate VDAC activity. Further genetic and molecular studies are required to uncover the detailed molecular mechanism by which presynaptic membrane VDAC regulates SV cycle in central synapses and NMJs.

Transparency document

The Transparency document associated with this article can be found, in online version.

CRediT authorship contribution statement

Guzalia F. Zakyrjanova:Investigation, Formal analysis, Visualization.**Amir I. Gilmutdinov**:Investigation, Formal analysis, Visualization.**Andrey N. Tsentsevitsky**:Investigation, Formal analysis, Visualization.**Alexey M. Petrov**:Conceptualization, Supervision, Writing - review & editing, Funding acquisition.

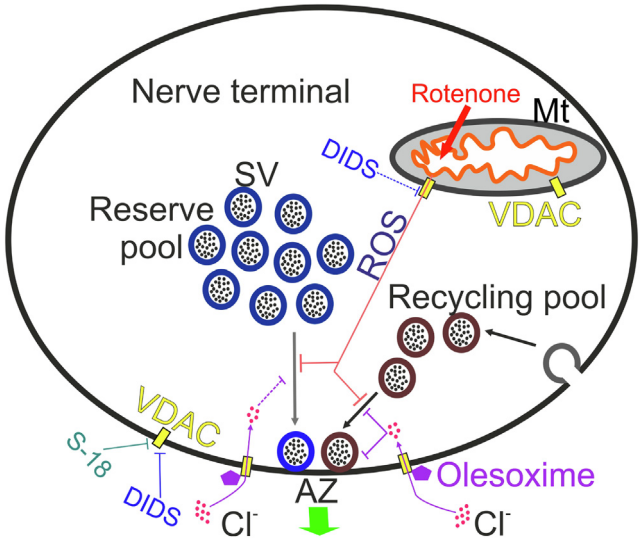

Fig. 5. Proposed mechanism for VDAC-dependent regulation of neurotransmitter release in NMJs. Stimulation of plasma membrane VDAC with olesoxime increases a permeability of the membrane for anion (Cl^-). An increased Cl^- flux into the nerve terminal can suppress evoked exocytosis of SVs and their mobilization from the recycling and reserve pools to exocytotic sites (active zone; AZ). Both cell-permeable (DIDS) and -impermeable (S-18) inhibitors of VDAC can completely abolish the effect of olesoxime on both SV exocytosis and intracellular Cl^- levels. Rotenone induces mitochondrial dysfunction that is associated with enhanced ROS production and mitochondrial permeability transition pore opening. This can disrupt an involvement of the SVs into evoked exocytosis. Inhibition of VDACs with cell-permeable compound DIDS can partially prevent the action of rotenone on mitochondrial ROS levels and SV mobilization. Olesoxime and S-18 do not counteract the effects of rotenone. These results suggest that olesoxime affects evoked SV exocytosis by acting on plasmallemal VDACs.

Declaration of competing interest

The authors declare that they have no known competing financial interests or personal relationships that could have appeared to influence the work reported in this paper.

Acknowledgements

We thank Prof. Andrey Zefirov (Kazan State Medical University) for comments and suggestions, Dr. Andrey Zakharov (Kazan Federal University) for excellent technical assistance. Also, we thank Reviewers for helpful comments. Author contributions: G. Z. A.G., and A.T. performed all experiments and analyzed. A.M.P. designed the research, interpreted results of experiments and wrote the manuscript. All the authors read and approved the final version of manuscript.

Funding

This study was supported in part by the Russian Foundation for Basic Research grant # 20-04-00077 (A.M.P) and partially the government assignment for FRC Kazan Scientific Center of RAS.

Appendix A. Supplementary data

Supplementary data to this article can be found online at https://doi.org/10.1016/j.bbalip.2020.158739.

References

[1] S.O. Rizzoli, Synaptic vesicle recycling: steps and principles, EMBO J. 33 (2014) 788–822.
[2] T. Maritzen, V. Haucke, Coupling of exocytosis and endocytosis at the presynaptic active zone, Neurosci. Res. 127 (2018) 45–52.
[3] S.V. Ovsepian, V.B. O'Leary, N.M. Ayvazyan, A. Al-Sabi, V. Ntziachristos, J.O. Dolly, Neurobiology and therapeutic applications of neurotoxins targeting transmitter release, Pharmacol. Ther. 193 (2019) 135–155.
[4] J.O. Dolly, G.W. Lawrence, J. Meng, J. Wang, S.V. Ovsepian, Neuro-exocytosis: botulinum toxins as inhibitory probes and versatile therapeutics, Curr. Opin. Pharmacol. 9 (2009) 326–335.
[5] B. Davletov, E. Ferrari, Y. Ushkaryov, Presynaptic neurotoxins: an expanding array of natural and modified molecules, Cell Calcium 52 (2012) 234–240.
[6] S.V. Ovsepian, V.B. O'Leary, L. Zaborszky, V. Ntziachristos, J.O. Dolly, Synaptic vesicle cycle and amyloid beta: biting the hand that feeds, Alzheimers Dement. 14 (2018) 502–513.
[7] S.V. Ovsepian, V.B. O'Leary, L. Zaborszky, V. Ntziachristos, J.O. Dolly, Amyloid plaques of Alzheimer's disease as hotspots of Glutamatergic activity, Neuroscientist 25 (2019) 288–297.
[8] T. Yasuda, Y. Nakata, C.J. Choong, H. Mochizuki, Neurodegenerative changes initiated by presynaptic dysfunction, Transl Neurodegener 2 (2013) 16.
[9] E. Lauwers, R. Goodchild, P. Verstreken, Membrane lipids in presynaptic function and disease, Neuron 90 (2016) 11–25.
[10] A.M. Petrov, M.R. Kasimov, A.L. Zefirov, Cholesterol in the pathogenesis of Alzheimer's, Parkinson's Diseases and Autism: link to synaptic dysfunction, Acta Naturae 9 (2017) 26–37.
[11] Y.C. Li, E.T. Kavalali, Synaptic vesicle-recycling machinery components as potential therapeutic targets, Pharmacol. Rev. 69 (2017) 141–160.
[12] A.M. Krivoi II, Petrov, Cholesterol and the Safety Factor for Neuromuscular Transmission, Int J Mol Sci, 20, (2019).
[13] O. Zamir, M.P. Charlton, Cholesterol and synaptic transmitter release at crayfish neuromuscular junctions, J. Physiol. 571 (2006) 83–99.
[14] C.R. Wasser, M. Ertunc, X. Liu, E.T. Kavalali, Cholesterol-dependent balance between evoked and spontaneous synaptic vesicle recycling, J. Physiol. 579 (2007) 413–429.
[15] A. Linetti, A. Fratangeli, E. Taverna, P. Valnegri, M. Francolini, V. Cappello, M. Matteoli, M. Passafaro, P. Rosa, Cholesterol reduction impairs exocytosis of synaptic vesicles, J. Cell Sci. 123 (2010) 595–605.
[16] G. Teixeira, L.B. Vieira, M.V. Gomez, C. Guatimosim, Cholesterol as a key player in the balance of evoked and spontaneous glutamate release in rat brain cortical synaptosomes, Neurochem. Int. 61 (2012) 1151–1159.
[17] A.M. Petrov, A.A. Yakovleva, A.L. Zefirov, Role of membrane cholesterol in spontaneous exocytosis at frog neuromuscular synapses: reactive oxygen species-calcium interplay, J. Physiol. 592 (2014) 4995–5009.
[18] A.M. Petrov, G.F. Zakyrjanova, A.A. Yakovleva, A.L. Zefirov, Inhibition of protein kinase C affects on mode of synaptic vesicle exocytosis due to cholesterol depletion, Biochem. Biophys. Res. Commun. 456 (2015) 145–150.
[19] A.M. Petrov, M.R. Kasimov, A.R. Giniatullin, O.I. Tarakanova, A.L. Zefirov, The role of cholesterol in the exo- and endocytosis of synaptic vesicles in frog motor nerve endings, Neurosci. Behav. Physiol. 40 (2010) 894–901.
[20] J.S. Dason, A.J. Smith, L. Marin, M.P. Charlton, Vesicular sterols are essential for synaptic vesicle cycling, J. Neurosci. 30 (2010) 15856–15865.
[21] H.Y. Yue, J. Xu, Cholesterol regulates multiple forms of vesicle endocytosis at a mammalian central synapse, J. Neurochem. 134 (2015) 247–260.
[22] A.M. Petrov, M.R. Kasimov, A.R. Giniatullin, A.L. Zefirov, Effects of oxidation of membrane cholesterol on the vesicle cycle in motor nerve terminals in the frog Rana Ridibunda, Neurosci. Behav. Physiol. 44 (2014) 1020–1030.
[23] M.R. Kasimov, M.R. Fatkhrakhmanova, K.A. Mukhutdinova, A.M. Petrov, 24S-Hydroxycholesterol enhances synaptic vesicle cycling in the mouse neuromuscular junction: implication of glutamate NMDA receptors and nitric oxide, Neuropharmacology 117 (2017) 61–73.
[24] K.A. Mukhutdinova, M.R. Kasimov, G.F. Zakyrjanova, M.R. Gumerova, A.M. Petrov, Oxysterol modulates neurotransmission via liver-X receptor/NO synthase-dependent pathway at the mouse neuromuscular junctions, Neuropharmacology 150 (2019) 70–79.
[25] K.A. Mukhutdinova, M.R. Kasimov, A.R. Giniatullin, G.F. Zakyrjanova, A.M. Petrov, 24S-hydroxycholesterol suppresses neuromuscular transmission in SOD1(G93A) mice: a possible role of NO and lipid rafts, Mol. Cell. Neurosci. 88 (2018) 308–318.
[26] M.R. Kasimov, G.F. Zakyrjanova, A.R. Giniatullin, A.L. Zefirov, A.M. Petrov, Similar oxysterols may lead to opposite effects on synaptic transmission: Olesoxime versus 5alpha-cholestan-3-one at the frog neuromuscular junction, Biochim. Biophys. Acta 1861 (2016) 606–616.
[27] M.R. Kasimov, A.R. Giniatullin, A.L. Zefirov, A.M. Petrov, Effects of 5alpha-cholestan-3-one on the synaptic vesicle cycle at the mouse neuromuscular junction, Biochim. Biophys. Acta 1851 (2015) 674–685.
[28] T.J. Nelson, D.L. Alkon, Insulin and cholesterol pathways in neuronal function, memory and neurodegeneration, Biochem. Soc. Trans. 33 (2005) 1033–1036.
[29] A.O. Sodero, J. Vriens, D. Ghosh, D. Stegner, A. Brachet, M. Pallotto, M. Sassoe-Pognetto, J.F. Brouwers, J.B. Helms, B. Nieswandt, T. Voets, C.G. Dotti, Cholesterol loss during glutamate-mediated excitotoxicity, EMBO J. 31 (2012) 1764–1773.
[30] F. Arenas, C. Garcia-Ruiz, J.C. Fernandez-Checa, Intracellular cholesterol trafficking and impact in Neurodegeneration, Front. Mol. Neurosci. 10 (2017) 382.
[31] A.M. Petrov, M.R. Kasimov, A.L. Zefirov, Brain cholesterol metabolism and its defects: linkage to neurodegenerative diseases and synaptic dysfunction, Acta Nat. 8 (2016) 58–73.
[32] A.M. Petrov, I.A. Pikuleva, Cholesterol 24-hydroxylation by CYP46A1: benefits of modulation for brain diseases, Neurotherapeutics 16 (2019) 635–648.
[33] B. Sottero, D. Rossin, E. Staurenghi, P. Gamba, G. Poli, G. Testa, Omics analysis of oxysterols to better understand their pathophysiological role, Free Radic. Biol. Med.

144 (2019) 55–71.
[34] T. Bordet, B. Buisson, M. Michaud, C. Drouot, P. Galea, P. Delaage, N.P. Akentieva, A.S. Evers, D.F. Covey, M.A. Ostuni, J.J. Lacapere, C. Massaad, M. Schumacher, E.M. Steidl, D. Maux, M. Delaage, C.E. Henderson, R.M. Pruss, Identification and characterization of cholest-4-en-3-one, oxime (TRO19622), a novel drug candidate for amyotrophic lateral sclerosis, J. Pharmacol. Exp. Ther. 322 (2007) 709–720.
[35] J.J. Weber, L.E. Clemensson, H.B. Schioth, H.P. Nguyen, Olesoxime in neurodegenerative diseases: Scrutinising a promising drug candidate, Biochem. Pharmacol. 168 (2019) 305–318.
[36] T. Bordet, P. Berna, J.L. Abitbol, R.M. Pruss, Olesoxime (TRO19622): a novel mitochondrial-targeted Neuroprotective compound, Pharmaceuticals (Basel) 3 (2010) 345–368.
[37] L.J. Martin, N.A. Adams, Y. Pan, A. Price, M. Wong, The mitochondrial permeability transition pore regulates nitric oxide-mediated apoptosis of neurons induced by target deprivation, J. Neurosci. 31 (2011) 359–370.
[38] A. Rovini, P.A. Gurnev, A. Beilina, M. Queralt-Martin, W. Rosencrans, M.R. Cookson, S.M. Bezrukov, T.K. Rostovtseva, Molecular mechanism of olesoxime-mediated neuroprotection through targeting alpha-synuclein interaction with mitochondrial VDAC, Cell. Mol. Life Sci. (2019), https://doi.org/10.1007/s00018-019-03386-w PMID: 31760463.
[39] F. Elinder, N. Akanda, R. Tofighi, S. Shimizu, Y. Tsujimoto, S. Orrenius, S. Ceccatelli, Opening of plasma membrane voltage-dependent anion channels (VDAC) precedes caspase activation in neuronal apoptosis induced by toxic stimuli, Cell Death Differ. 12 (2005) 1134–1140.
[40] R. Marin, C.M. Ramirez, M. Gonzalez, E. Gonzalez-Munoz, A. Zorzano, M. Camps, R. Alonso, M. Diaz, Voltage-dependent anion channel (VDAC) participates in amyloid beta-induced toxicity and interacts with plasma membrane estrogen receptor alpha in septal and hippocampal neurons, Mol. Membr. Biol. 24 (2007) 148–160.
[41] C.M. Ramirez, M. Gonzalez, M. Diaz, R. Alonso, I. Ferrer, G. Santpere, B. Puig, G. Meyer, R. Marin, VDAC and ERalpha interaction in caveolae from human cortex is altered in Alzheimer's disease, Mol. Cell. Neurosci. 42 (2009) 172–183.
[42] M.I. Bahamonde, J.M. Fernandez-Fernandez, F.X. Guix, E. Vazquez, M.A. Valverde, Plasma membrane voltage-dependent anion channel mediates antiestrogen-activated maxi cl- currents in C1300 neuroblastoma cells, J. Biol. Chem. 278 (2003) 33284–33289.
[43] M.I. Bahamonde, M.A. Valverde, Voltage-dependent anion channel localises to the plasma membrane and peripheral but not perinuclear mitochondria, Pflugers Arch. 446 (2003) 309–313.
[44] M.A. Baker, D.J. Lane, J.D. Ly, V. De Pinto, A. Lawen, VDAC1 is a transplasma membrane NADH-ferricyanide reductase, J. Biol. Chem. 279 (2004) 4811–4819.
[45] A.M. Rahbar, C. Fenselau, Integration of Jacobson's pellicle method into proteomic strategies for plasma membrane proteins, J. Proteome Res. 3 (2004) 1267–1277.
[46] V. De Pinto, A. Messina, D.J. Lane, A. Lawen, Voltage-dependent anion-selective channel (VDAC) in the plasma membrane, FEBS Lett. 584 (2010) 1793–1799.
[47] M. Gonzalez-Gronow, R. Ray, F. Wang, S.V. Pizzo, The voltage-dependent anion channel (VDAC) binds tissue-type plasminogen activator and promotes activation of plasminogen on the cell surface, J. Biol. Chem. 288 (2013) 498–509.
[48] L. Li, Y.C. Yao, X.Q. Gu, D. Che, C.Q. Ma, Z.Y. Dai, C. Li, T. Zhou, W.B. Cai, Z.H. Yang, X. Yang, G.Q. Gao, Plasminogen kringle 5 induces endothelial cell apoptosis by triggering a voltage-dependent anion channel 1 (VDAC1) positive feedback loop, J. Biol. Chem. 289 (2014) 32628–32638.
[49] M. Morciano, T. Beckhaus, M. Karas, H. Zimmermann, W. Volknandt, The proteome of the presynaptic active zone: from docked synaptic vesicles to adhesion molecules and maxi-channels, J. Neurochem. 108 (2009) 662–675.
[50] M. Lassek, J. Weingarten, W. Volknandt, The proteome of the murine presynaptic active zone, Proteomes 2 (2014) 243–257.
[51] W. Volknandt, M. Karas, Proteomic analysis of the presynaptic active zone, Exp. Brain Res. 217 (2012) 449–461.
[52] M. Morciano, J. Burre, C. Corvey, M. Karas, H. Zimmermann, W. Volknandt, Immunoisolation of two synaptic vesicle pools from synaptosomes: a proteomics analysis, J. Neurochem. 95 (2005) 1732–1745.
[53] S. Takamori, M. Holt, K. Stenius, E.A. Lemke, M. Gronborg, D. Riedel, H. Urlaub, S. Schenck, B. Brugger, P. Ringler, S.A. Muller, B. Rammner, F. Grater, J.S. Hub, B.L. De Groot, G. Mieskes, Y. Moriyama, J. Klingauf, H. Grubmuller, J. Heuser, F. Wieland, R. Jahn, Molecular anatomy of a trafficking organelle, Cell 127 (2006) 831–846.
[54] E. Benítez-Rangel, M.C. López-Méndez, L. García, A. Guerrero-Hernández, DIDS (4,4′-Diisothiocyanatostilbene-2,2′-Disulfonate) Directly Inhibits Caspase Activity in HeLa Cell Lysates, Cell Death Discovery, 1, (2015).
[55] D. Ben-Hail, V. Shoshan-Barmatz, VDAC1-interacting anion transport inhibitors inhibit VDAC1 oligomerization and apoptosis, Biochim. Biophys. Acta 1863 (2016) 1612–1623.
[56] C.A. Stein, M. Colombini, Specific VDAC inhibitors: phosphorothioate oligonucleotides, J. Bioenerg. Biomembr. 40 (2008) 157–162.
[57] W. Tan, J.C. Lai, P. Miller, C.A. Stein, M. Colombini, Phosphorothioate oligonucleotides reduce mitochondrial outer membrane permeability to ADP, Am J Physiol Cell Physiol 292 (2007) C1388–C1397.
[58] N. Li, K. Ragheb, G. Lawler, J. Sturgis, B. Rajwa, J.A. Melendez, J.P. Robinson, Mitochondrial complex I inhibitor rotenone induces apoptosis through enhancing mitochondrial reactive oxygen species production, J. Biol. Chem. 278 (2003) 8516–8525.
[59] T. Searl, C. Prior, I.G. Marshall, Acetylcholine recycling and release at rat motor nerve terminals studied using (−)-vesamicol and troxpyrrolium, J. Physiol. 444 (1991) 99–116.
[60] A.V. Zakharov, Elph: An Open-Source Program for Acquisition Control and Analysis of Electrophysiological Signals, Seriya Estestvennye Nauki 161 Uchenye Zapiski Kazanskogo Universiteta, 2019, pp. 245–254.
[61] W.J. Betz, G.S. Bewick, Optical monitoring of transmitter release and synaptic vesicle recycling at the frog neuromuscular junction, J. Physiol. 460 (1993) 287–309.
[62] A.M. Petrov, A.R. Giniatullin, G.F. Sitdikova, A.L. Zefirov, The role of cGMP-dependent signaling pathway in synaptic vesicle cycle at the frog motor nerve terminals, J. Neurosci. 28 (2008) 13216–13222.
[63] U.G. Odnoshivkina, V.I. Sytchev, L.F. Nurullin, A.R. Giniatullin, A.L. Zefirov, A.M. Petrov, β2-adrenoceptor agonist-evoked reactive oxygen species generation in mouse atria: implication in delayed inotropic effect, Eur. J. Pharmacol. 765 (2015) 140–153.
[64] J. Biwersi, A.S. Verkman, Cell-permeable fluorescent indicator for cytosolic chloride, Biochemistry 30 (2002) 7879–7883.
[65] N. Chub, G.Z. Mentis, M.J. O'Donovan, Chloride-sensitive MEQ fluorescence in Chick embryo Motoneurons following manipulations of chloride and during spontaneous network activity, J. Neurophysiol. 95 (2006) 323–330.
[66] A. Godbole, J. Varghese, A. Sarin, M.K. Mathew, VDAC is a conserved element of death pathways in plant and animal systems, Biochimica et Biophysica Acta (BBA) - Molecular Cell Research 1642 (2003) 87–96.
[67] S.O. Rizzoli, W.J. Betz, Synaptic vesicle pools, Nat. Rev. Neurosci. 6 (2005) 57–69.
[68] A.L. Zefirov, A.V. Zakharov, R.D. Mukhametzyanov, A.M. Petrov, G.F. Sitdikova, The vesicle cycle in motor nerve endings of the mouse diaphragm, Neurosci. Behav. Physiol. 39 (2009) 245–252.
[69] I. Shafir, W. Feng, V. Shoshan-Barmataz, J. Bioenerg. Biomembr. 30 (1998) 499–510.
[70] D.A. Richards, C. Guatimosim, S.O. Rizzoli, W.J. Betz, Synaptic vesicle pools at the frog neuromuscular junction, Neuron 39 (2003) 529–541.
[71] C. Chauvin, F. De Oliveira, X. Ronot, M. Mousseau, X. Leverve, E. Fontaine, Rotenone inhibits the mitochondrial permeability transition-induced cell death in U937 and KB cells, J. Biol. Chem. 276 (2001) 41394–41398.
[72] B. Landolfi, S. Curci, L. Debellis, T. Pozzan, A.M. Hofer, Ca2+ homeostasis in the agonist-sensitive internal store: functional interactions between mitochondria and the ER measured in situ in intact cells, J. Cell Biol. 142 (1998) 1235–1243.
[73] A. Raghavan, T. Sheiko, B.H. Graham, W.J. Craigen, Voltage-dependant anion channels: novel insights into isoform function through genetic models, Biochim. Biophys. Acta Biomembr. 1818 (2012) 1477–1485.
[74] T. Becker, R. Wagner, Mitochondrial Outer Membrane Channels: Emerging Diversity in Transport Processes, BioEssays, 40, (2018).
[75] S.M. Stevens Jr., A.D. Zharikova, L. Prokai, Proteomic analysis of the synaptic plasma membrane fraction isolated from rat forebrain, Brain Res. Mol. Brain Res. 117 (2003) 116–128.
[76] B.A. Jordan, B.D. Fernholz, M. Boussac, C. Xu, G. Grigorean, E.B. Ziff, T.A. Neubert, Identification and verification of novel rodent postsynaptic density proteins, Mol. Cell. Proteomics 3 (2004) 857–871.
[77] G.R. Phillips, L. Florens, H. Tanaka, Z.Z. Khaing, L. Fidler, J.R. Yates 3rd, D.R. Colman, Proteomic comparison of two fractions derived from the transsynaptic scaffold, J. Neurosci. Res. 81 (2005) 762–775.
[78] X. Xiong, S. Huang, H. Zhang, J. Li, J. Shen, J. Xiong, Y. Lin, L. Jiang, X. Wang, S. Liang, Enrichment and proteomic analysis of plasma membrane from rat dorsal root ganglions, Proteome Sci. 7 (2009) 41.
[79] B.P. Weiser, R. Salari, R.G. Eckenhoff, G. Brannigan, Computational investigation of cholesterol binding sites on mitochondrial VDAC, J. Phys. Chem. B 118 (2014) 9852–9860.
[80] W.W.L. Cheng, M.M. Budelier, Y. Sugasawa, L. Bergdoll, M. Queralt-Martin, W. Rosencrans, T.K. Rostovtseva, Z.W. Chen, J. Abramson, K. Krishnan, D.F. Covey, J.P. Whitelegge, A.S. Evers, Multiple neurosteroid and cholesterol binding sites in voltage-dependent anion channel-1 determined by photo-affinity labeling, Biochim. Biophys. Acta Mol. Cell Biol. Lipids 1864 (2019) 1269–1279.
[81] A.M. Petrov, V.V. Kravtsova, V.V. Matchkov, A.N. Vasiliev, A.L. Zefirov, A.V. Chibalin, J.A. Heiny, I.I. Krivoi, Membrane lipid rafts are disturbed in the response of rat skeletal muscle to short-term disuse, Am J Physiol Cell Physiol 312 (2017) C627–C637.
[82] A.M. Petrov, K.E. Kudryashova, Y.G. Odnoshivkina, A.L. Zefirov, Cholesterol and lipid rafts in the plasma membrane of nerve terminal and membrane of synaptic vesicles, Neurochem. J. 5 (2011) 13–19.
[83] B.H. Graham, Z. Li, E.P. Alesii, P. Versteken, C. Lee, J. Wang, W.J. Craigen, Neurologic dysfunction and male infertility in Drosophila porin mutants: a new model for mitochondrial dysfunction and disease, J. Biol. Chem. 285 (2010) 11143–11153.
[84] D. Pathak, L.Y. Shields, B.A. Mendelsohn, D. Haddad, W. Lin, A.A. Gerencser, H. Kim, M.D. Brand, R.H. Edwards, K. Nakamura, The role of mitochondrially derived ATP in synaptic vesicle recycling, J. Biol. Chem. 290 (2015) 22325–22336.
[85] S.V. Hrynevich, T.G. Pekun, T.V. Waseem, S.V. Fedorovich, Influence of glucose deprivation on membrane potentials of plasma membranes, mitochondria and synaptic vesicles in rat brain synaptosomes, Neurochem Res 40 (2015) 1188–1196.
[86] M.V. Ivannikov, M. Sugimori, R.R. Llinas, Synaptic vesicle exocytosis in hippocampal synaptosomes correlates directly with total mitochondrial volume, J. Mol. Neurosci. 49 (2013) 223–230.
[87] M.S. Lustgarten, A. Bhattacharya, F.L. Muller, Y.C. Jang, T. Shimizu, T. Shirasawa, A. Richardson, H. Van Remmen, Complex I generated, mitochondrial matrix-directed superoxide is released from the mitochondria through voltage dependent anion channels, Biochem. Biophys. Res. Commun. 422 (2012) 515–521.
[88] M. Gonzalez-Gronow, T. Kalfa, C.E. Johnson, G. Gawdi, S.V. Pizzo, The voltage-dependent anion channel is a receptor for plasminogen kringle 5 on human endothelial cells, J. Biol. Chem. 278 (2003) 27312–27318.
[89] S.F. Okada, W.K. O'Neal, P. Huang, R.A. Nicholas, L.E. Ostrowski, W.J. Craigen,

E.R. Lazarowski, R.C. Boucher, Voltage-dependent anion channel-1 (VDAC-1) contributes to ATP release and cell volume regulation in murine cells, J Gen Physiol 124 (2004) 513–526.
[90] R. Darbandi-Tonkabon, B.D. Manion, W.R. Hastings, W.J. Craigen, G. Akk, J.R. Bracamontes, Y. He, T.V. Sheiko, J.H. Steinbach, S.J. Mennerick, D.F. Covey, A.S. Evers, Neuroactive steroid interactions with voltage-dependent anion channels: lack of relationship to GABA(a) receptor modulation and anesthesia, J. Pharmacol. Exp. Ther. 308 (2004) 502–511.
[91] S. Dadsena, S. Bockelmann, J.G.M. Mina, D.G. Hassan, S. Korneev, G. Razzera, H. Jahn, P. Niekamp, D. Muller, M. Schneider, F.G. Tafesse, S.J. Marrink, M.N. Melo, J.C.M. Holthuis, Ceramides bind VDAC2 to trigger mitochondrial apoptosis, Nat. Commun. 10 (2019) 1832.
[92] D.C. Crawford, S. Mennerick, Presynaptically silent synapses: dormancy and awakening of presynaptic vesicle release, Neuroscientist 18 (2012) 216–223.
[93] S. Sugita, L.L. Fleming, C. Wood, S.K. Vaughan, M.P. Gomes, W. Camargo, L.A. Naves, V.F. Prado, M.A. Prado, C. Guatimosim, G. Valdez, VAChT overexpression increases acetylcholine at the synaptic cleft and accelerates aging of neuromuscular junctions, Skelet. Muscle 6 (2016) 31.
[94] E. Tremblay, E. Martineau, R. Robitaille, Opposite synaptic alterations at the neuromuscular junction in an ALS mouse model: when motor units matter, J. Neurosci. 37 (2017) 8901–8918.
[95] O.P. Edupuganti, S.V. Ovsepian, J. Wang, T.H. Zurawski, J.J. Schmidt, L. Smith, G.W. Lawrence, J.O. Dolly, Targeted delivery into motor nerve terminals of inhibitors for SNARE-cleaving proteases via liposomes coupled to an atoxic botulinum neurotoxin, FEBS J. 279 (2012) 2555–2567.
[96] S.V. Ovsepian, V.B. O'Leary, V. Ntziachristos, J.O. Dolly, Circumventing brain barriers: Nanovehicles for Retroaxonal therapeutic delivery, Trends Mol. Med. 22 (2016) 983–993.
[97] S.V. Ovsepian, M. Bodeker, V.B. O'Leary, G.W. Lawrence, J. Oliver Dolly, Internalization and retrograde axonal trafficking of tetanus toxin in motor neurons and trans-synaptic propagation at central synapses exceed those of its C-terminal-binding fragments, Brain Struct. Funct. 220 (2015) 1825–1838.